Monthly Notices
of the
ROYAL ASTRONOMICAL SOCIETY

MNRAS **443,** 2444–2451 (2014) doi:10.1093/mnras/stu1335

An extensive photometric study of the recently discovered intermediate polar V647 Aur (1RXS J063631.9+353537)

V. P. Kozhevnikov★

Astronomical Observatory, Ural Federal University, Lenin Av. 51, Ekaterinburg 620083, Russia

Accepted 2014 July 2. Received 2014 July 2; in original form 2014 June 3

ABSTRACT

We report the results of photometry of the intermediate polar V647 Aur. Observations were obtained over 42 nights in 2012 and 2013. The total duration of the observations was 246 h. We clearly detected three oscillations with periods of 932.9123 ± 0.0011, 1008.307 97 ± 0.000 38 and 1096.955 ± 0.004 s, which may be the white dwarf spin period and two orbital sidebands, respectively. The oscillation with a period of 932.9123 s has a quasi-sinusoidal pulse profile with a slightly changeable semi-amplitude from 10.9 mmag in 2012 to 12.5 mmag in 2013. The oscillation with a period of 1008.307 97 s has a slightly asymmetric pulse profile with a remarkable small hump on the ascending part. The semi-amplitude of this oscillation is highly changeable both in a time-scale of days (26–77 mmag) and in a time-scale of years (47 mmag in 2012 and 34 mmag in 2013). The oscillation with a period of 1096.955 s has a highly asymmetric pulse profile with a semi-amplitude of about 6 mmag. The three detected oscillations imply an orbital period of 3.465 65 ± 0.000 06 h. By comparing our data with the data of Gänsicke et al., which were obtained eight years ago, we discovered that the spin period of the white dwarf in V647 Aur decreases with $\mathrm{d}P/\mathrm{d}t = (-1.36 \pm 0.08) \times 10^{-10}$. This important result should be confirmed by future observations. Our oscillation ephemerides and times of maxima can be useful for this confirmation.

Key words: stars: individual: V647 Aur – novae, cataclysmic variables – stars: oscillations.

1 INTRODUCTION

Intermediate polars (IPs) form a sub-class of cataclysmic variables (CVs), in which a magnetic white dwarf accretes material from a late-type companion filling its Roche lobe. The rotation of the white dwarf is not phase locked to the binary period of the system. Because the magnetic axis is offset from the spin axis of the white dwarf, this causes oscillations in the X-ray and optical wavelength bands. The X-ray oscillation period is usually identified as the spin period of the white dwarf. In addition to the spin and orbital periods, the reprocessing of X-rays at some part of the system that rotates with the orbital period gives rise to emission that varies with the beat period, where $1/P_{\rm beat} = 1/P_{\rm spin} - 1/P_{\rm orb}$. This synodic counterpart is often called the orbital sideband of the spin frequency or $\omega - \Omega$, where $\omega = 1/P_{\rm spin}$ and $\Omega = 1/P_{\rm orb}$. Other orbital sidebands such as $\omega - 2\Omega$ and $\omega + \Omega$ can be additionally observed (Warner 1986). A comprehensive review of IPs is given in Patterson (1994).

Gänsicke et al. (2005) reported the results from a search of CVs using a combined X-ray (*ROSAT*) and infrared (2MASS) target selection. They found four new IPs. One of them was denominated V647 Aur. Gänsicke et al. detected two optical oscillations with periods of 1008.3408 ± 0.0019 and 930.5829 ± 0.0040 s. In addition, from radial velocity measurements, Gänsicke et al. found $P_{\rm orb}$ = 201 ± 8 min. Recently, Shears & Miller (2011) confirmed the larger period, which turned out equal to 1008.3 ± 0.5 s. However, until lately in the IP home page (http://asd.gsfc.nasa.gov/Koji.Mukai/iphome), this IP was reckoned among probable IPs but not among confirmed or ironclad IPs, because there was no X-ray confirmation of the period. This problem might be solved due to recent X-ray observations of V647 Aur reported by Bernardini et al. (2012). They, however, detected the X-ray periods, which were incompatible with the periods found by Gänsicke et al. (2005) and Shears & Miller (2011). Thus, the X-ray observations reported by Bernardini et al. made V647 Aur a puzzling star rather than a confirmed IP.

We made a trial photometric observation of V647 Aur and discovered that it showed a short-period oscillation directly in the light curve. This oscillation was also easily detectable in the power spectrum. Therefore, V647 Aur should be a no-problem star. Moreover, due to large amplitude, the period of this oscillation can be measured with high precision allowing long-term tracking of period

★E-mail: valery.kozhevnikov@urfu.ru

changes. To obtain the oscillation period with high precision and derive an oscillation ephemeris with a long validity, we performed extensive photometric observations of V647 Aur. In this paper, we present results of all our observations, spanning a total duration of 246 h within 42 nights.

2 OBSERVATIONS

In observations of CVs, we use a multichannel photometer that allows us to make continuous brightness measurements of two stars and the sky background. Because the angular separation between the programme and comparison stars is small, such differential photometry allows us to obtain magnitudes, which are corrected for first-order atmospheric extinction and for other unfavourable atmospheric effects (unstable atmospheric transparency, light absorption by thin clouds, etc.). Moreover, we use the CCD guiding system, which enables precise centring of the two stars in the diaphragms to be maintained automatically. This greatly facilitates the acquisition of long continuous light curves and improves the accuracy of brightness measurements. The design of the photometer is described in Kozhevnikov & Zakharova (2000).

V647 Aur was observed in 2012 January–March and December, and in 2013 January–March over 42 nights using the 70-cm telescope at Kourovka Observatory, Ural Federal University. A journal of the observations is given in Table 1. Below, for brevity, the data obtained in 2012 December are ascribed to the data obtained in 2013. The programme and comparison stars were observed through 16-arcsec diaphragms, and the sky background was observed through a 30-arcsec diaphragm. The comparison star is USNO-A2.0 1200-04971757. It has $\alpha = 06^{\rm h}36^{\rm m}41\overset{\rm s}{.}48$, $\delta = +35^{\circ}\,31'\,54\overset{''}{.}86$ and $B = 14.6$ mag. Data were collected at 8-s sampling intervals in white light (approximately 300–800 nm), employing a PC-based data-acquisition system.

We obtained differences of magnitudes of the programme and comparison stars taking into account the differences in light sensitivity between the various channels. According to the mean counts, the photon noise (rms) of the differential light curves is equal to 0.09–0.11 mag (a time resolution of 8 s). The actual rms noise also includes atmospheric scintillations and the motion of the star images in the diaphragms. But these noise components give only insignificant additions. Fig. 1 presents the longest differential light curves of V647 Aur, with magnitudes averaged over 64-s time intervals. The white-noise component of these light curves is 0.03–0.04 mag.

Table 1. Journal of the observations.

Date (UT)	HJD start (−2450000)	Length (h)
2012 January 24	5951.316444	6.3
2012 January 25	5952.134132	10.1
2012 January 26	5953.164534	9.0
2012 January 27	5954.120988	7.9
2012 January 28	5955.102313	5.1
2012 February 11	5969.120096	4.6
2012 February 12	5970.118565	6.1
2012 February 13	5971.118094	7.8
2012 February 14	5972.118568	8.7
2012 February 15	5973.119849	9.2
2012 February 16	5974.118626	9.3
2012 February 17	5975.123681	7.3
2012 February 18	5976.132078	6.4
2012 February 24	5982.135324	8.0
2012 February 25	5983.137418	8.0
2012 March 11	5998.199233	2.8
2012 March 12	5999.156396	5.3
2012 March 14	6001.234320	1.9
2012 March 16	6003.171543	4.4
2012 March 17	6004.165672	2.2
2012 December 16	6278.321162	5.6
2012 December 18	6280.252442	2.5
2012 December 19	6281.302231	5.6
2013 January 3	6296.126082	6.5
2013 January 7	6300.300209	5.6
2013 January 11	6304.095021	11.0
2013 January 16	6309.215073	8.7
2013 January 17	6310.268036	2.6
2013 January 18	6311.289039	3.2
2013 February 2	6326.229786	3.0
2013 February 3	6327.256329	2.4
2013 February 7	6331.153087	4.5
2013 February 8	6332.117132	8.0
2013 February 12	6336.119761	1.8
2013 February 16	6340.166383	7.3
2013 March 1	6353.137689	4.1
2013 March 3	6355.215228	4.7
2013 March 4	6356.143816	3.3
2013 March 6	6358.173664	6.5
2013 March 11	6363.152900	6.9
2013 March 13	6365.154998	6.5
2013 March 14	6366.159642	5.5

3 ANALYSIS AND RESULTS

As seen in Fig. 1, the light curves of V647 Aur are fairly typical of CVs in showing rapid flickering. Moreover, a periodic oscillation is directly visible in the light curves. Fig. 2 presents the amplitude spectra calculated by a fast Fourier transform algorithm for the longest light curves of V647 Aur. Previously, low-frequency trends were removed from the light curves by subtraction of a second-order polynomial fit. The amplitude spectra reveal that the oscillation has a large semi-amplitude of about 40 mmag, which is changeable from night to night, and a period of 1008 s.

One of the amplitude spectra (Fig. 2), namely 2012 February 16, hints at the first harmonic of the 1008-s oscillation. The average power spectrum, however, did not reveal noticeable first and second harmonics of the 1008-s oscillation. This means that the pulse profile of the 1008-s oscillation is simple and smooth.

A distinctive feature of the periodic oscillations seen in IPs is their coherence. Analysing the data incorporated into common time series, the coherence can be demonstrated due to coincidence of the structure of the power spectrum and the window function. Fig. 3 presents the Fourier power spectra of two common time series consisting of the data obtained in 2012 and 2013. The gaps due to daylight and poor weather in these time series were filled with zeros. Previously, low-frequency trends were removed from the individual light curves by subtraction of a first- or second-order polynomial fit. As seen in Fig. 3, the 1008-s oscillation reveals distinct pictures closely resembling the window functions obtained from artificial time series consisting of a sine wave and the gaps according to the observations. This proves the coherence of the oscillation over the corresponding time intervals. Due to the presence of 1-d aliases, the power spectra shown in Fig. 3 allow us to detect one more coherent oscillation with much lesser amplitude.

Schwarzenberg-Czerny (1991) showed that the 1σ confidence interval of the oscillation period is the width of the peak in the power spectrum at the $p - N^2$ level, where p is the peak height and N^2 is the mean noise power level. We used this method to evaluate

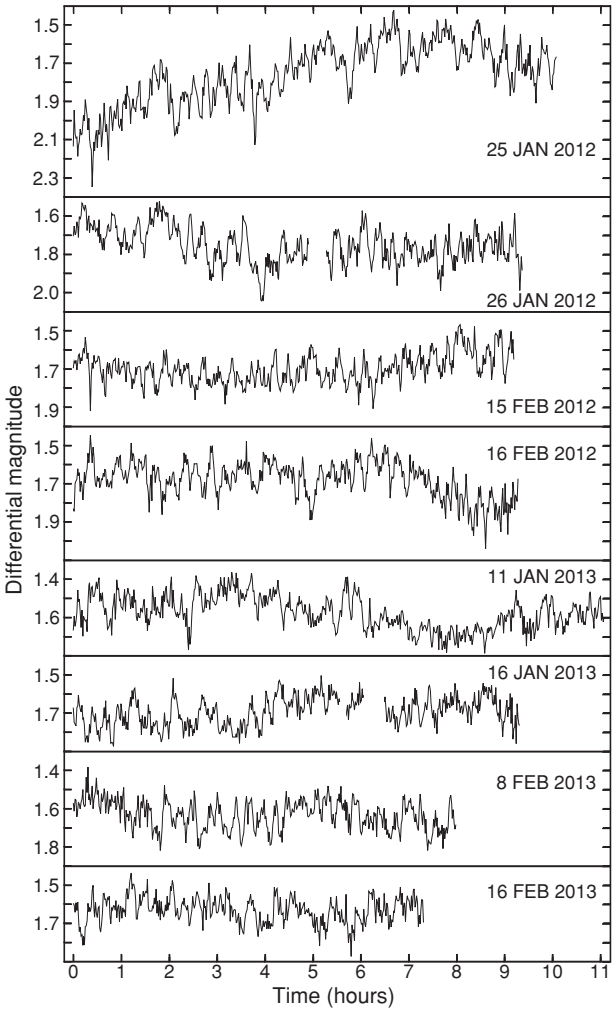

Figure 1. Longest differential light curves of V647 Aur.

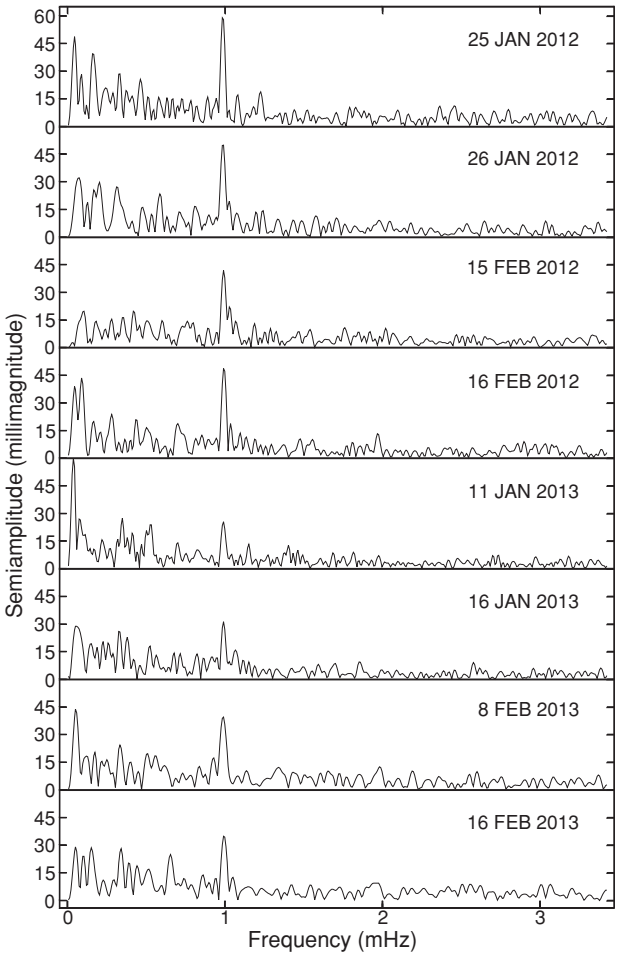

Figure 2. Amplitude spectra of V647 Aur. The prominent peak visible in the amplitude spectra has a period of 1008 s.

the precision of the oscillation periods. The precise maxima of the principal peaks were found by a Gaussian function fitted to the upper parts of the peaks. From the power spectra presented in Fig. 3, we found $P_1 = 1008.3103 \pm 0.0061$ s and $P_2 = 932.900 \pm 0.016$ s in 2012, and $P_1 = 1008.3056 \pm 0.0042$ s and $P_2 = 932.917 \pm 0.009$ s in 2013.

Obviously, the highest precision of oscillation periods can be achieved from all data incorporated into common time series. The Fourier power spectrum calculated for all data from V647 Aur (Fig. 4) showed the distinct principal peaks well separated from different aliases for both detected oscillations. This means that our data are quite densely spaced in time, and the aliasing problem is absent. The close resemblance of the power spectrum in the vicinities of the two oscillations with the window function proves their coherence during 14 months. From this power spectrum, we obtained $P_1 = 1008.307\,97 \pm 0.000\,38$ s and $P_2 = 932.9127 \pm 0.0011$ s.

To obtain high sampling of the Fourier power spectra, we added a considerable number of zeros at the end of the common time series. For the power spectrum of all the data, the sampling that might allow us to measure the peak width turned out to be extremely high, and this power spectrum consisted of 2^{25} points. To exclude any gross errors, which might be related with this giant number of points, we also calculated the power spectrum by a sine wave fitted to the light curves folded with trial frequencies. In addition, we used the analysis-of-variance method (Schwarzenberg-Czerny 1989). By using these methods, we obtained the periods nearly identical to the periods obtained from the Fourier power spectrum.

The power spectra (Fig. 3) show an enlarged noise level in the vicinity of the oscillation with P_1. This suggests the presence of additional oscillations. To find this out, we used the well-known method of subtraction of the largest oscillation from data. Indeed, the residual power spectrum (Fig. 5) allowed us to detect one more coherent oscillation. This oscillation is obvious due to the presence of 1-d aliases. This third oscillation has the period $P_3 = 1096.955 \pm 0.004$ s and a semi-amplitude of about 0.006 mag.

The oscillation with P_3 is quite distant in frequency from the oscillation with P_1. None the less, this oscillation is affected by the oscillation with P_1. This suggests that the oscillation with P_2 can also be affected by the oscillation with P_1. To find this out, we performed numerical experiments with artificial time series and found that, due to relatively small amplitude, the oscillation with P_2 was noticeably sensitive to the influence of the oscillation with P_1. Therefore, we remeasured the period P_2 from the pre-whitened data and found that it was equal to 932.909 ± 0.016 s in 2012, 932.916 ± 0.009 s in 2013 and 932.9123 ± 0.0011 s in all the data.

Summarized information about the periods and amplitudes of the oscillations with P_1 and P_2 obtained in different seasons is given in Tables 2 and 3. The precise semi-amplitudes and their rms errors were found from a sine wave fitted to folded light curves. In

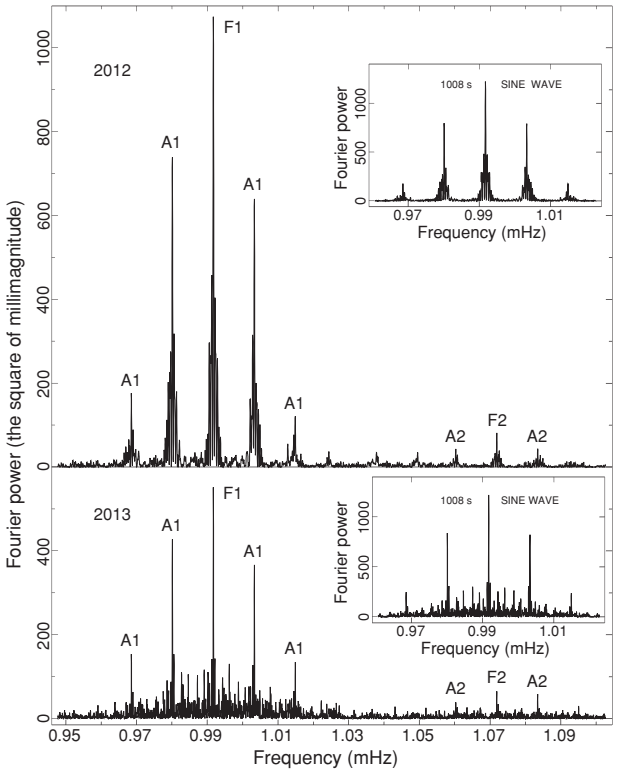

Figure 3. Power spectra calculated for the data of 2012 and 2013 from V647 Aur. They reveal two coherent oscillations with the periods $P_1 = 1008.31$ s and $P_2 = 932.9$ s. Inserted frames show the window functions. The principal peaks are labelled with 'F1' and 'F2', and the 1-d aliases are labelled with 'A1' and 'A2'.

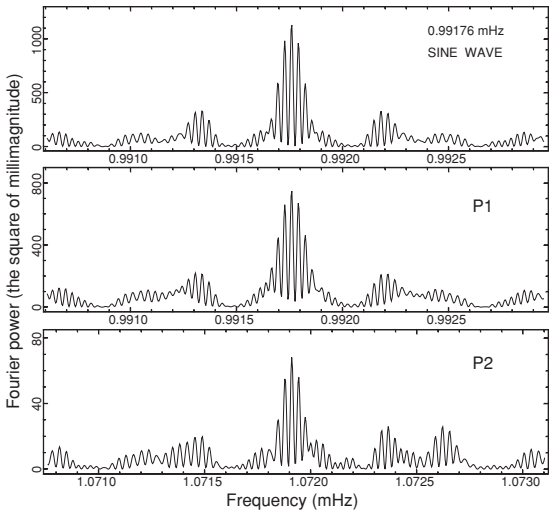

Figure 4. Segments of the power spectrum calculated for all data from V647 Aur. They cover the vicinities of the periods P_1 and P_2. The upper frame shows the window function.

addition, in the fourth columns we give the half-width of the peaks at half-maximum (HWHM), which is often used as a conservative error, and in the fifth columns we give the rms errors according to Schwarzenberg-Czerny (1991). One can notice that the rms errors are considerably less than the conservative errors, where this difference increases with length of the observations. Obviously, growth of the precision occurs due to both the increase of the frequency resolution and the decrease of the relative noise level. Because the errors of the periods found from all the data are much lower than the other errors, we found the deviations of the other periods and expressed them in units of their rms errors. This is shown in the sixth columns of Tables 2 and 3. All the deviations are less than the rms errors. This means that the rms errors may be somewhat overestimated.

The individual light curves have low frequency resolution and are suitable only for the determination of the phases of the oscillation with P_1, which has a much larger amplitude. However, for the light curves 3–6 h long, the relative noise can be considerable when the oscillation with P_1 diminishes its amplitude. Therefore, for the determination of the phases, we used the light curves longer than 6.9 h (3100 points). They were folded with P_1. To precisely find the times of maxima, we used a sine wave fitted to folded light curves. Results of these phase measurements together with the oscillation semi-amplitudes found from the sine waves fitted are given in Table 4. Accepting the time of maximum of the first light curve as the initial time, we derived the following tentative ephemeris:

$$\mathrm{HJD(max\ 1)} = 2455952.14659(7) + 0.0116702311(44). \quad (1)$$

According to this ephemeris, we calculated the observed minus calculated (O−C) values and numbers of the oscillation cycles, and presented them in Table 4. The (O−C) values revealed an obvious slope. However, it seems premature to correct the ephemeris, because, as seen in Table 4, the number of (O−C) values in 2013 is considerably less than that in 2012, and their errors of times of maxima are larger due to less amplitude. Therefore, we decided to derive another ephemeris, for which, to obtain times of maxima, larger parts of data are used.

Although the individual light curves are not suitable to obtain times of maxima of the oscillation with P_2 due to its low amplitude, this seems possible by using large parts of data. Obviously, in this case, it is necessary to use pre-whitened data. By using large parts of data, we derived both ephemeris for the oscillation with P_1 and that with P_2. We found the initial times of maxima from the data of 2012 and utilized the data of 2013 for verification. In addition, we subdivided the data into four groups (see Tables 5 and 6) and also used them for verification. To precisely find the times of maxima and oscillation semi-amplitudes, we also used a sine wave fitted to folded light curves. Because the times of maxima were obtained from the folded light curves of large parts of data, we refer these times to the middle of corresponding observations. Finally, for the oscillations with P_1 and P_2, we obtained the following ephemerides:

$$\mathrm{HJD(max\ 1)} = 2455977.797720(40) + 0.0116702311(44) \quad (2)$$

$$\mathrm{HJD(max\ 2)} = 2455977.79905(9) + 0.010797596(13). \quad (3)$$

According to these ephemerides, we calculated the (O−C) values and numbers of the oscillation cycles, and presented them in Tables 5 and 6 and in Fig. 6. As seen, the (O−C) diagrams reveal only very small slopes. These slopes are much less than their rms errors. Hence, the ephemerides cannot be corrected.

The time during which the accumulated error from the period runs up to one oscillation cycle is considered as a formal validity of an ephemeris. The formal validities of the ephemerides of the oscillations with P_1 and with P_2 are 85 and 27 yr, respectively (a 1σ confidence level). In the second case, the diminishing of the formal validity is caused by less oscillation amplitude and accordingly larger relative noise level.

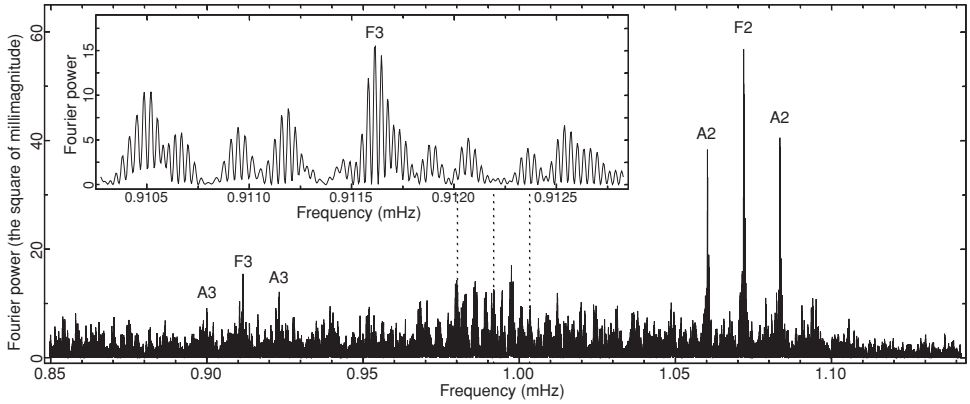

Figure 5. Power spectrum of all data of V647 Aur, from which the largest oscillation was subtracted. It allows us to detect one more oscillation with the period P_3. The inserted frame shows the surrounding of the principal peak of the oscillation with P_3 on an expanded scale. The dotted lines mark the location of the principal peak of the subtracted oscillation and its 1-d aliases. The 1-d aliases of the oscillations with P_2 and P_3 are labelled with 'A2' and 'A3', respectively.

Table 2. The values and precisions of the period P_1.

Time span	Semi-amp. (mmag)	Period (s)	HWHM (s)	Error σ (s)	Dev.
2012	47 ± 1	1008.3103	0.1090	0.0061	0.4σ
2013	34 ± 1	1008.3056	0.0540	0.0042	0.9σ
Total	41 ± 1	1008.307 97	0.008 33	0.000 38	–

Table 3. The values and precisions of the period P_2.

Time span	Semi-amp. (mmag)	Period (s)	HWHM (s)	Error σ (s)	Dev.
2012	10.9 ± 0.6	932.909	0.083	0.016	0.2σ
2013	12.5 ± 0.6	932.916	0.039	0.009	0.4σ
Total	11.7 ± 0.5	932.9123	0.0071	0.0011	–

Table 4. Verification of the ephemeris of the oscillation with P_1 by using longest individual light curves.

Date (UT)	Semi-amp. (mmag)	HJD(max) (−2450000)	No. of cycles	O−C (s)
2012 January 25	58 ± 2	5952.14659(7)	0	–
2012 January 26	50 ± 3	5953.17363(10)	88	5 ± 10
2012 January 27	59 ± 3	5954.13043(8)	170	-9 ± 9
2012 February 13	46 ± 3	5971.13377(11)	1627	-25 ± 11
2012 February 14	76 ± 2	5972.12605(6)	1712	2 ± 8
2012 February 15	42 ± 2	5973.12952(9)	1798	-12 ± 10
2012 February 16	49 ± 3	5974.13338(11)	1884	7 ± 11
2012 February 17	28 ± 3	5975.13658(16)	1970	-31 ± 15
2012 February 24	47 ± 2	5982.15063(9)	2571	-11 ± 10
2012 February 25	40 ± 2	5983.15427(9)	2657	-10 ± 10
2013 January 11	26 ± 3	6304.10903(20)	30 159	-5 ± 18
2013 January 16	32 ± 2	6309.23246(12)	30 598	12 ± 12
2013 February 8	40 ± 3	6332.12914 (15)	32 560	-15 ± 14
2013 February 16	35 ± 2	6340.18135(12)	33 250	-36 ± 12
2013 March 11	40 ± 3	6363.16017(12)	35 219	-25 ± 12

Fig. 7 presents the light curves of V647 Aur folded with the periods $P_1 = 1008.307\,97$ s, $P_2 = 932.9123$ s and $P_3 = 1096.955$ s. The oscillation with P_1 has a slightly asymmetric pulse profile with a small remarkable hump in phases 0.2–0.35, where this hump is observable both in the data of 2012 and in the data of 2013. The oscillation with P_2 reveals a quasi-sinusoidal pulse profile.

Table 5. Verification of the ephemeris of the oscillation with P_1 by using large parts of data.

Time span	HJD(max) (−245 0000)	No. of cycles	O−C (s)
2012 January 24–February 14	5961.90286(4)	–1362	-0.3 ± 5
2012 February 15–March 17	5988.69772(5)	934	0.2 ± 6
2012 December 16–2013 February 3	6302.84881(4)	27 853	12 ± 5
2013 February 7–March 14	6348.77093(6)	31 788	-8 ± 6
2013 all	6322.36131(4)	29 525	2 ± 5

Table 6. Verification of the ephemeris of the oscillation with P_2.

Time span	HJD(max) (−245 0000)	No. of cycles	O−C (s)
2012 January 24–February 14	5961.90505(10)	–1472	5 ± 12
2012 February 15–March 17	5988.69373(17)	1009	-8 ± 16
2012 December 16–2013 February 3	6302.83906(11)	30 103	-2 ± 12
2013 February 7–March 14	6348.78287(13)	34 358	1 ± 13
2013 all	6322.361 13(9)	31 911	0.5 ± 11

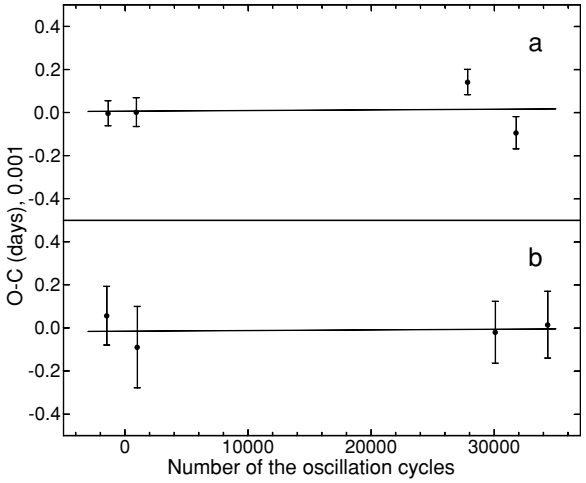

Figure 6. O−C diagrams for all data from V647 Aur that are subdivided into four groups and folded with the periods P_1 (a) and P_2 (b).

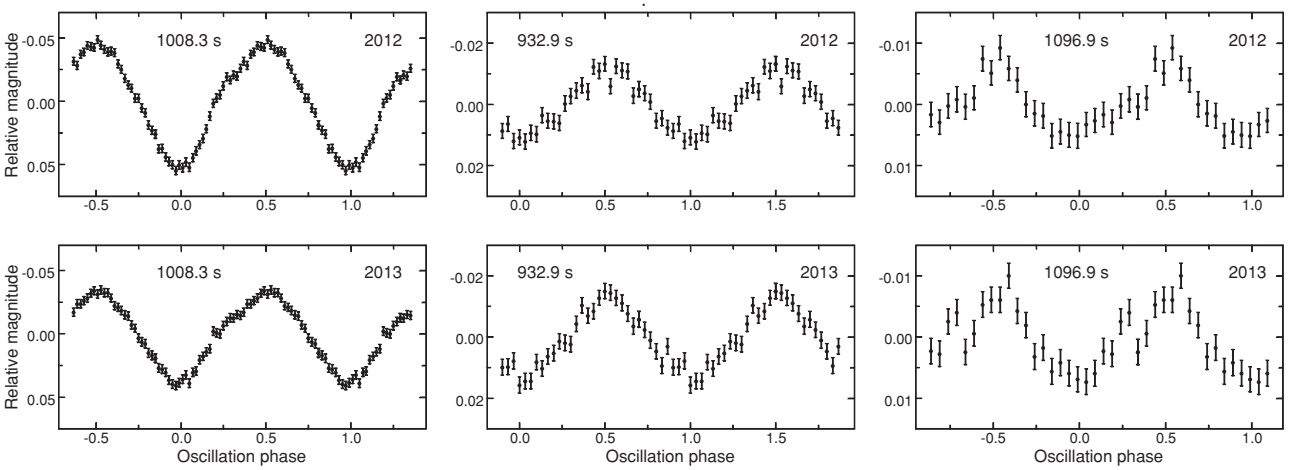

Figure 7. Pulse profiles of three oscillations obtained for the data of 2012 and 2013 from V647 Aur. The oscillation with a period of 1008.307 97 s (on the right) has a slightly asymmetric pulse profile with changeable amplitude and a small hump in phases 0.2–0.35. The oscillation with a period of 932.9123 s (in the middle) has a quasi-sinusoidal pulse profile. The oscillation with a period of 1096.955 s (on the right) reveals a highly asymmetric pulse profile with a slow rise to maximum and a rapid decline to minimum.

The oscillation with P_3 reveals a highly asymmetric pulse profile with a slow rise to maximum and a rapid decline to minimum.

The three detected oscillations are equally spaced in frequency. Obviously, they conform to the spin period and two orbital sidebands. Then, from the most precise periods P_1 and P_2, we derive the precise orbital period, which is equal to $3.465\,65 \pm 0.000\,06$ h. This period coincides with the orbital period found by Gänsicke et al. (2005) from radial velocity measurements (3.35 ± 0.13 h). However, we could not find the orbital period in our data. This suggests that the orbital inclination of V647 Aur is less than 50° (e.g. la Dous 1994).

4 DISCUSSION

We performed extensive photometric observations of V647 Aur with a total duration of 246 h in 2012 and 2013, and clearly found three highly coherent oscillations with the periods $P_1 = 1008.307\,97 \pm 0.000\,38$ s, $P_2 = 932.9123 \pm 0.0011$ s and $P_3 = 1096.955 \pm 0.004$ s. On average, the semi-amplitude of the oscillation with P_1 is 41 mmag, but it is highly changeable both in a time-scale of days and in a time-scale of years (see Tables 2 and 4). In contrast, the oscillation with P_2 reveals only small changes of its amplitude in a time-scale of years (see Table 3). On average, its semi-amplitude is 11.7 mmag. The semi-amplitude of the oscillation with P_3 is roughly 6 mmag and appears stable. This third oscillation was detected by us for the first time.

Two optical oscillations that certify V647 Aur as an IP were discovered by Gänsicke et al. (2005). We found, however, that only one of their periods is close to our 1008-s period. Another period, which is equal to 930.5829 ± 0.0040 s, does not agree with our shortest period. The difference is 2.3 s. To realize the reason for this large difference, we simulated the observations of V647 Aur by Gänsicke et al. according to their table 1 and found that, due to unfavourable distribution of the observations in time with a large four-month gap, the oscillation with P_2 is highly affected by the oscillation with P_1. Therefore, Gänsicke et al. could not achieve high precision of the period of this oscillation without pre-whitening. But they did not mention about such a method.

These numerical experiments demonstrated that the oscillation with P_2 cannot considerably affect the oscillation with P_1. Therefore, the larger period found by Gänsicke et al. seems reliable. It is equal to 1008.3408 ± 0.0019 s and also differs from our 1008-s period, where the difference is 0.0328 s (17σ). Because this difference is not too large, we can attribute it to the change of $P_{\rm spin}$. Dividing this difference by the middle time interval between the observations by Gänsicke et al. and our observations, which is 7.6 yr, we derive $\mathrm{d}P/\mathrm{d}t = (-1.36 \pm 0.08) \times 10^{-10}$.

Gänsicke et al. gave the times of maxima for their eight light curves of V647 Aur (see their table 4). Therefore, we can check $\mathrm{d}P/\mathrm{d}t$ by using the following formula (Breger & Pamyatnykh 1998):

$$(\mathrm{O}-\mathrm{C}) = 0.5\,\frac{1}{p}\,\frac{\mathrm{d}P}{\mathrm{d}t}\,t^2. \qquad (4)$$

From our ephemeris, we obtained inconsistent values of (O−C). The average (O−C) values were equal to $+320 \pm 39$ s for four nights in 2004 October and -319 ± 8 s for four nights in 2005 February–March. Obviously, the (O−C) values exceeded one oscillation cycle. Indeed, according to $\mathrm{d}P/\mathrm{d}t$, the (O−C) value becomes equal to one oscillation cycle in 3.9 yr. Supposing that the true (O−C) value comprises three oscillation cycles plus the observed (O−C) value, two values of $\mathrm{d}P/\mathrm{d}t$ derived from the times of maxima in 2004 October and in 2005 February–March can be agreed. They are equal to -1.26×10^{-10} and -1.12×10^{-10}, respectively. The average difference between the $\mathrm{d}P/\mathrm{d}t$ found from the times of maxima and the $\mathrm{d}P/\mathrm{d}t$ found from the difference of periods is less than 2.1σ. This seems a good concord and proves reality of the period change.

Gänsicke et al. could not decide which of the two periods is $P_{\rm spin}$. The recent X-ray observations of V647 Aur presented by Bernardini et al. (2012) can help to solve this question. They found three X-ray periods. Two of them, which are equal to 920 ± 1 and 952 ± 4 s, were attributed to $P_{\rm spin}$ and $\omega - \Omega$, respectively. These periods, however, are incompatible with the optical periods. Moreover, the orbital period being derived from the two X-ray periods, which is equal to 7.6 ± 0.9 h, is also incompatible with the orbital period found by Gänsicke et al. Obviously, this total incompatibility signifies an error.

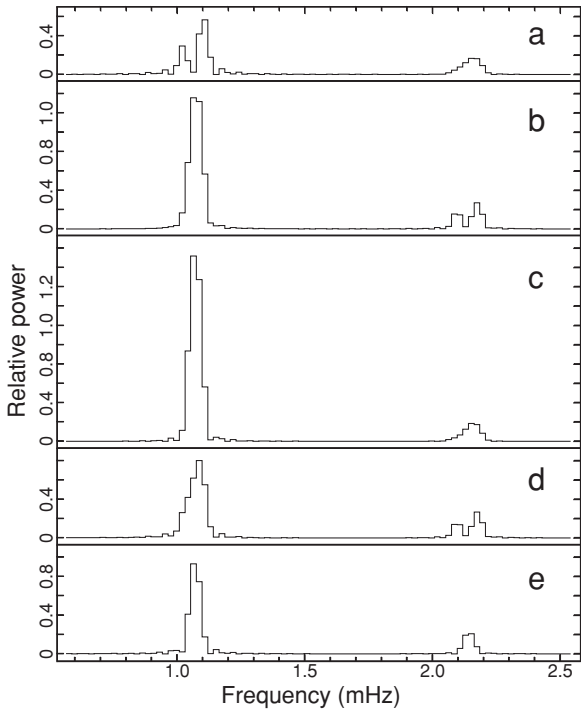

Figure 8. Power spectra which characterize interaction of two oscillations in short time series. The initial phase differences are 0.2 (a), 0.5 (b), 0.7 (c) and 0.0 (d). Panel (e) shows the power spectrum of a short time series consisting of a single sine wave with a 933-s period, to which a high-frequency harmonic was added.

To realize the reason for this incompatibility, we simulated the X-ray observations of V647 Aur. We constructed artificial time series consisting of two sine waves with the periods and amplitudes according to table 2 in Bernardini et al. and with changeable initial phase differences. In fact, these phase differences are the phases of the beat period between the two sine waves. A high-frequency harmonic with half-amplitude was added to each of these sine waves. The length of these time series was 4.75 h, which is the net exposure times minus the solar flare removed exposure according to table 1 in Bernardini et al. Fig. 8 presents typical Fourier power spectra calculated with frequency bins of 0.0222 mHz (which are seen in the X-ray power spectrum of V647 Aur). The effects of interaction of two oscillations in short time series turned out quite diverse. Depending on the included phases of the beat period, two oscillations can be resolved (Fig. 8a) or unresolved (Figs 8b and c). Moreover, the peak can be asymmetric and thus hinting at two oscillations (Fig. 8d). The probability of this particular case is rather low and is equal roughly to 1/5.

Bernardini et al. suspected two oscillations due to asymmetry of the peak in the X-ray power spectrum (see their fig. 3). Indeed, two oscillations with the suggested periods and amplitudes can produce a single asymmetric peak with a rather low probability. But this peak must be more wide than seen in the X-ray power spectrum if the length of the observations is 4.75 h (Fig. 8d). Hence, the asymmetry of the peak in the X-ray power spectrum must be attributed to noise rather than the two oscillations. Moreover, the high-frequency harmonic visible in the X-ray power spectrum conforms also to a single oscillation because, otherwise, the corresponding peak must be either noticeably wider or resolved into two components. Obviously, Bernardini et al. also believe that this peak conforms to a single oscillation because, in their fig. 3, it is labelled with '2ω'. Directly from the X-ray power spectrum of V647 Aur presented in fig. 3 in Bernardini et al., we found that the first harmonic is equal to 2.141 ± 0.011 mHz. Here, the error is half of the frequency bin. Then, $P_{\rm spin}$ is equal to 934 ± 5 s and conforms pretty well to P_2. Note that latter conclusion remains valid even if the X-ray observations are longer than 4.75 h.

Bernardini et al. reported detection of the third X-ray oscillation in V647 Aur, insisting that it is $\omega - 2\Omega$. However, they themselves recognize that their estimated orbital period (7.6 h) is inconsistent with $\omega - 2\Omega$ (see p. 8 in Bernardini et al.). We found that the period corresponding to the left blue dotted line denoting $\omega - 2\Omega$ in fig. 3 in Bernardini et al. is equal to 1014 ± 11 s. This period also conforms pretty well to P_1. Thus, the careful inspection of the X-ray power spectrum convinces that it shows only two periods rather than three periods, where these periods coincide with the optical periods. Then, we conclude that P_2 is $P_{\rm spin}$ because it coincides with the shortest X-ray period having the largest X-ray amplitude. Consequently, the oscillation with P_1 is $\omega - \Omega$, and the oscillation with P_3 is $\omega - 2\Omega$.

Two-pole disc-fed accretion is believed to be the normal mode of behaviour in IPs. Depending on the sizes of the accretion curtains, both single-peaked and double-peaked spin pulse profiles can be produced. In IPs with strong magnetic fields, two accreting poles can act in phase so that single-picked, roughly sinusoidal pulse profiles can be produced, whereas in IPs with weak magnetic fields, two accreting poles can act in anti-phase and produce double-peaked spin pulse profiles (Norton et al. 1999). It is considered that the rapidly spinning IPs with $P_{\rm spin} < 700$ s have weak magnetic fields and therefore usually produce double-peaked pulse profiles (Norton et al.). According to $P_{\rm spin}$, V647 Aur must have a strong magnetic field and, therefore, it must show a quasi-sinusoidal spin pulse profile. This conception agrees with the quasi-sinusoidal pulse profile of the oscillation with P_2.

In the case of disc-fed accretion, the optical orbital sideband arises due to reprocessing of X-rays by structures rotating in the reference frame connected with the orbital motion. In particular, reprocessing can occur in asymmetric parts of the disc. V647 Aur shows highly changeable amplitude of the sideband oscillation. Large changes of the sideband amplitude in a time-scale of days are especially surprising (see Table 4). These changes are not accompanied by variations of the star brightness (Fig. 1) and hence by changes of the structure of the disc. Moreover, these changes are not accompanied by changes of the amplitude of the oscillation with $P_{\rm spin}$. Therefore, the sideband oscillation in V647 Aur is difficult to account for through reprocessing.

Another way to produce the orbital sideband is alternation of the accretion flow between two poles of the white dwarf with the sideband frequency. This process occurs in the cases of stream-fed and disc-overflow accretion and is the only way to produce the strong orbital sideband in X-rays (Wynn & King 1992). The change of the contribution between the disc-overflow accretion and disc-fed accretion was observed in FO Aqr (Evans et al. 2004) and MU Cam (Staude et al. 2008). Although this change in MU Cam was accompanied by a large change in optical brightness, such changes seem possible without brightness changes, because the disc-overflow accretion can amount to only a small part of the full accretion (e.g. Mukai, Ishida & Osborne 1994). The amplitude of the sideband modulation of V647 Aur in X-rays is relatively small and does not indicate inevitably disc-overflow accretion. None the less, we can account for the optical orbital sideband and changes of its amplitude in V647 Aur by disc-overflow accretion, because

the contribution of disc-overflow accretion can probably change without brightness changes.

Norton, Wynn & Somerscales (2004) used a model of magnetic accretion to investigate the spin equilibria of magnetic CVs. This allowed them to infer approximate values for the magnetic moments of most known IPs. Many authors used their fig. 2 to evaluate the magnetic moments of newly discovered IPs (e.g. Rodríguez-Gil et al. 2005; Katajainen et al. 2010). We also found the place of V647 Aur in fig. 2 in Norton et al. and the corresponding magnetic moment, which is equal to 1×10^{33} G cm^3. By considering properties of its nearest near-by IPs, which are V2004 Oph, BG CMi, FO Aqr and MU Cam, we, however, discovered that these IPs have different magnetic fields and show different accretion modes. Indeed, BG CMi and V2004 Oph represent rare cases, showing circular polarization and indicating thus strong magnetic field (Katajainen et al. 2007, 2010), whereas FO Aqr represents the counterexample with probably less strong magnetic field because of non-detection of circular polarization (Stockman et al. 1992). None the less, FO Aqr possesses disc-overflow accretion similar to that observed in MU Cam and BG CMi (Norton et al. 1992). However, unlike the three IPs, V2004 Oph exhibits pure stream-fed accretion due to more strong magnetic field (Hellier & Beardmore 2002). The reason for this discrepancy may consist in substantial deviation from spin equilibrium. Indeed, FO Aqr is the only IP, which clearly demonstrates the spin equilibrium by alternating spin-up and spin-down (Kruszewski & Semeniuk 1998; Patterson et al. 1998; Williams 2003). Other sparse IPs, in which spin period changes were observed, show either continuous spin-up or continuous spin-down (Kruszewski & Semeniuk 1998).

We found that V647 Aur reveals decreasing of $P_{\rm spin}$ with $\mathrm{d}P/\mathrm{d}t = (-1.36 \pm 0.08) \times 10^{-10}$. This change is close to the largest period changes detected in other IPs (see table 1 in Warner 1996), and also close to the period change lately observed in FO Aqr ($\mathrm{d}P/\mathrm{d}t = -2.0 \times 10^{-10}$; Williams 2003). Being a new result, the spin period change in V647 Aur should be confirmed by future observations. This can be made by using our ephemerides and by using our times of maxima. We note that the large $\mathrm{d}P/\mathrm{d}t$ observed in V647 Aur facilitates possible detection of alternating spin-up and spin-down.

5 CONCLUSIONS

We performed extensive photometric observations of V647 Aur over 42 nights in 2012 and 2013. The total duration of the observations was 246 h.

(i) The analysis of these data allowed us to clearly detect three coherent oscillations with the periods $P_1 = 1008.307\,97 \pm 0.000\,38$ s, $P_2 = 932.9123 \pm 0.0011$ s and $P_3 = 1096.955 \pm 0.004$ s. The shortest period is the spin period of the white dwarf. Two other periods correspond to its two negative orbital sidebands.

(ii) These three oscillations imply that the orbital period of the system is equal to $3.465\,65 \pm 0.000\,06$ h.

(iii) The oscillation with P_1 has a slightly asymmetric pulse profile with a small hump in the ascending part. The oscillation with P_2 has a quasi-sinusoidal pulse profile. The oscillation with P_3 reveals a highly asymmetric pulse profile.

(iv) The high precision of two periods allowed us to obtain the oscillation ephemerides with formal validities of 85 yr for the oscillation with P_1 and of 27 yr for the oscillation with P_2.

(v) By comparing our data with the data obtained by Gänsicke et al. (2005) eight years ago, we discovered that V647 Aur exhibits the period decrease with $\mathrm{d}P/\mathrm{d}t = (-1.36 \pm 0.08) \times 10^{-10}$.

ACKNOWLEDGEMENTS

This research has made use of the SIMBAD data base, operated at CDS, Strasbourg, France. This research also made use of the NASA Astrophysics Data System (ADS).

REFERENCES

Bernardini F., de Martino D., Falanga M., Mukai K., Matt G., Bonnet-Bidaud J. M., Masetti N., Mouchet M., 2012, A&A, 542, A22
Breger M., Pamyatnykh A. A., 1998, A&A, 332, 958
Evans P. A., Hellier C., Ramsay G., Cropper M., 2004, MNRAS, 349, 715
Gänsicke B. T. et al., 2005, MNRAS, 361, 141
Hellier C., Beardmore A. P., 2002, MNRAS, 331, 407
Katajainen S., Butters O. W., Norton A. J., Lehto H. J., Piirola V., 2007, A&A, 475, 1011
Katajainen S., Butters O., Norton A. J., Lehto H. J., Piirola V., Berdyugin A., 2010, ApJ, 724, 165
Kozhevnikov V. P., Zakharova P. E., 2000, in Garzon F., Eiroa C., de Winter D., Mahoney T. J., eds, ASP Conf. Ser. Vol. 219, Disks, Planetesimals and Planets. Astron. Soc. Pac., San Francisco, p. 381
Kruszewski A., Semeniuk I., 1998, Acta Astron., 48, 757
la Dous C., 1994, Space Sci. Rev., 67, 1
Mukai K., Ishida M, Osborne J. P., 1994, PASJ, 46, L87
Norton A. J., McHardy I. M., Lehto H. J., Watson M. G., 1992, MNRAS, 258, 697
Norton A. J., Beardmore A. P., Allan A., Hellier C., 1999, A&A, 347, 203
Norton A. J., Wynn G. A., Somerscales R. V., 2004, ApJ, 614, 349
Patterson J., 1994, PASP, 106, 209
Patterson J. et al., 1998, PASP, 110, 415
Rodríguez-Gil P. et al., 2005, A&A, 440, 701
Schwarzenberg-Czerny A., 1989, MNRAS, 241, 153
Schwarzenberg-Czerny A., 1991, MNRAS, 253, 198
Shears J., Miller I., 2011, J. Br. Astron. Assoc., 121, 161
Staude A., Schwope A. D., Schwarz R., Vogel J., Krumpe M., Nebot Gomez-Moran A., 2008, A&A, 486, 899
Stockman H. S., Schmidt G. D., Berriman G., Liebert J., Moore L. R., Wickramasinghe D. T., 1992, ApJ, 401, 628
Warner B., 1986, MNRAS, 219, 347
Warner B., 1996, Ap&SS, 241, 263
Williams G., 2003, PASP, 115, 618
Wynn G. A., King A. R., 1992, MNRAS, 255, 83

This paper has been typeset from a TEX/LATEX file prepared by the author.